A NOVEL MOORING TETHER FOR HIGHLY DYNAMIC OFFSHORE APPLICATIONS; MITIGATING PEAK AND FATIGUE LOADS VIA SELECTABLE AXIAL STIFFNESS

T.Gordelier, D.Parish, L.Johanning and P.R.Thies, *University of Exeter, UK*

ABSTRACT

Highly dynamic floating bodies such as wave energy convertors (WECs) require mooring lines with particular mechanical properties; the mooring system must achieve adequate station keeping whilst controlling mooring tensions within acceptable limits. Currently, fibre ropes are commonly used but many mooring designers are seeking alternative solutions that can offer more favourable mechanical properties.

The compliance offered by a mooring system will depend largely on the axial stiffness of the mooring lines. Whilst fibre ropes can offer lower axial stiffness than alternatives such as chain and wire rope, there remains a fundamental conflict which prohibits the free selection of axial stiffness properties. This conflict exists because the axial stiffness is strongly governed by the minimum breaking load (MBL) of the rope. The specified MBL must be sufficient to accommodate the predicted peak tension loads with an appropriate factor of safety (FOS) to cater for uncertainties and degradations. In achieving a sufficient MBL, the designer is often forced to accept a higher axial stiffness than is preferred. A potential benefit of reducing the axial stiffness of a mooring line is the reduction of peak loads and fatigue loads. This allows a reduction in mass of both the floating body and the mooring system, thus reducing costs and improving system reliability.

This work describes the 'Exeter Tether', an innovation in mooring tether design which decouples the axial stiffness properties from the MBL of the tether. Removing this constraint allows a tether to be specified according to both MBL and axial stiffness. The principles behind the novel tether design are introduced here, along with an outline of 5 prototype tether variants manufactured in collaboration with Lankhorst Ropes. Results from the proof of concept tests at the University of Exeter's Dynamic Marine Component Test Facility (DMaC) are presented together with preliminary findings from sea trials at the South West Moorings Test Facility (SWMTF). The anticipated load mitigation introduced via the mooring tether is investigated and the implications for system design are discussed.

1. INTRODUCTION

The mooring system is one of the most critical sub-systems for a floating offshore installation. In particular, marine renewable energy developers seek to install devices in highly dynamic environments governed by wave and tidal conditions. The requirements and design issues are extensively described by [1-3]. Importantly, mooring systems must satisfy the following requirements:

1. Survivability under extreme load conditions.
2. Long-term reliability.
3. Provision of required compliance so as to minimise peak loads.
4. Minimise the mooring spread footprint.

As a consequence, items 1 and 2 typically require a high Minimum Breaking Load (MBL), to allow sufficiently high factors of safety (FOS) to warrant long-term reliability. For conventional mooring systems both requirements conflict with objectives 3 & 4 and vice versa. The cost of conventional mooring line material (e.g. chain, steel wire and polyester) is directly proportional to the rated MBL [4]. As a consequence any peak loads, such as those experienced during storm events, have a direct impact on the mooring cost. The dilemma for floating offshore installations is that the capital cost of the mooring system is driven by extreme (peak load) conditions, whilst the revenue is generated under normal operating conditions. If peak loads can be mitigated the cost of mooring systems and associated structural elements, as well as deployment and installation costs, can be significantly reduced.

The design challenge is to find a feasible combination of all four objectives listed above. The key parameters to be mindful of are the combination of compliance and associated MBL.

Wave buoys typically feature a highly elastic mooring configuration using rubber materials [5]. This satisfies the design requirements for wave buoys to follow the orbital wave motion (item 3 above), whilst absorbing some of the wave and tide-induced forces to increase system reliability (item 2 above).

At the other end of the spectrum are taut mooring systems using steel wire, which are one of the proposed solutions for floating offshore wind mooring systems [6, 7]. The compliance of these systems is minimal and very high MBLs are required to satisfy item 1 (survivability). A combination of soft and stiff response elements would reconcile the different design objectives.

A number of systems are proposed to combine these characteristics, among which are the Seaflex buoy mooring system [8] and the TfI mooring tether [9, 10]. The development and proof of concept for a third innovative mooring design, the Exeter Tether, is the subject of this paper.

As for all innovative systems the performance characteristics and long-term behaviour require careful consideration, research and demonstration.

2. TECHNICAL BACKGROUND

2.1 AXIAL STIFFNESS, MAXIMUM STRAIN AND MIMIMUM BREAKING LOAD

Three important properties of a mooring line that strongly influence its performance [4] are:

2.1 (a) Axial stiffness in tension

This parameter describes the extension of a line in relation to its original length, when it is subjected to a given tensile load. A line with high stiffness (low compliance), for instance steel wire or steel chain, will not yield much when a load is applied [11]. This high stiffness can lead to excessively high ‘snatch’ loads being generated within the mooring system which are transmitted into the floating structure [4].

Axial stiffness is defined as *load (N) / strain*, or the gradient of the *load (N) / strain* plot line.

2.1 (b) Minimum breaking load

The minimum breaking load (MBL) under tension is specified for any rope, chain or similar structural tie. This value can be considered to be the least value at which a rope, chain or other will fail completely. Some permanent damage or change might occur at a lower load.

2.1 (c) Maximum limit of axial strain

This defines the maximum extension that a line can achieve before breaking at MBL. Conventional fibre ropes can achieve a maximum strain of around 0.40 (nylon, 3-strand laid construction, new rope) [12]. The ability to achieve high values of strain can be useful where large displacements must be allowed e.g. when tide height varies significantly in relation to the water depth.

In conventional fibre ropes the axial stiffness and MBL are strongly associated parameters. Consequently there is little capability to vary the stiffness of any particular rope, these parameters being governed by the MBL. Some selection of stiffness for a given MBL is possible by means of the following:

- Material selection

Fibre rope for offshore mooring might be of polyester, nylon, high modulus polyethylene or other polymer construction. The different polymer yarns exhibit differing extension and recovery properties; nylon has the lowest stiffness [12].

- Construction geometry

Fibre rope for offshore use can be constructed such that the main load carrying sub-ropes run either parallel to the rope itself (parallel lay), are helically wound within the rope (3-strand laid), or those that approximate a helical form, such as braided or plaited ropes. Ropes with parallel lay sub-ropes will exhibit higher stiffness than ropes where the load is carried helically [12].

The lowest axial stiffness for any given MBL of conventional fibre rope will therefore be achieved with a nylon rope. However, the advantageous maximum strain of 0.4 is only available at loads approaching the MBL of the rope. If a factor of safety is applied, to allow for uncertainties in the load case and degradations to the rope, the axial stiffness increases with the increase to MBL.

2.2 THE EXETER TETHER

The Exeter Tether [13, 14] is a tether assembly comprising a hollow braided fibre rope, an elastomeric core and at least one anti-friction membrane between the rope and the core (see Figure 1).

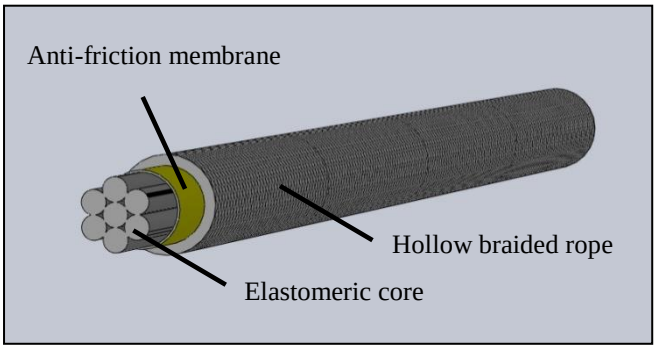

Figure 1: Representation of the Exeter Tether assembly

The tension load exerted onto the tether is carried solely by the hollow rope which is terminated with an eye splice at each end. As the rope extends, its diameter contracts according to the pitch angle of the braid. The elastomeric core resists this diametric change and in so doing, controls the extension of the tether. Design changes to the rope's pitch angle and to the compressibility of the core affect the resulting extension properties of the tether. Importantly though, these two properties can be changed independently of the inherent strength of any given hollow rope such that the extension properties of the tether are not coupled to its MBL. This allows the selection, at tether design stage, of lower axial stiffness and a higher strain limit whilst specifying the MBL to allow an adequate factor of safety.

3. PROOF OF CONCEPT PROTOTYPES

Prototype tethers were constructed for the proof of concept study and are referred to as the P1 series prototypes. The elastomer cores, together with their anti-friction membranes, were assembled by University of Exeter (UoE). These core assemblies were then taken to Lankhorst Ropes manufacturing facility in Maia, Portugal, where the rope was braided onto the cores and the eye splices were made. The completed tether assemblies were then shipped back to UoE for test work and analysis.

12 tether variants were manufactured in the P1 series; this paper will cover preliminary results for five of these tethers P1-2, P1-3, P1-4, P1-5 and P1-6.

3.1 CORE CONSTRUCTION

The core architecture as detailed in Figure 1 comprises a seven strand bundle of Ø25 mm section cords. The elastomer material used for the P1 series is ethylene propylene diene monomer (EPDM). The five variants of the tether introduced in this paper are constructed from EPDM with specified durometer hardness values of 50, 60, 70, 80 and 90 Shore A.

3.2 ANTI-FRICTION MEMBRANE

The anti-friction membrane serves two purposes: Initially the membrane binds the elastomer core assembly together providing some limited structural integrity prior to over-braiding with hollow rope; in service the membrane offers a lower friction surface for the rope strands to move across. A third benefit to be investigated is the potential resistance to marine growth developing within the core bundle.

3.3 HOLLOW ROPE

The material chosen for the hollow rope was polyester. The construction was a 1 x 1 braid of 48 strands (24 in each helix direction) with a strand diameter of 4.5 mm, Figure 2.

Figure 2: The 48 strand 1x1 braided rope (LH image) and Lankhorst Rope's A3 eye splice (RH image)

The braiding machine was set to produce a 200 mm pitch helix for each strand. The resulting outer diameter of the hollow rope was 60 mm which increased to approximately 85 mm when braiding onto a core assembly which was fed into the rear of the machine. The hollow rope was terminated at both ends using a form of Lankhorst Rope's A3 eye splice (Figure 2).

3.4 TETHER ASSEMBLIES

The construction and identification of the P1 series of prototypes described in this paper is detailed in Table 1. The dimensions of the tether are detailed in Figure 3.

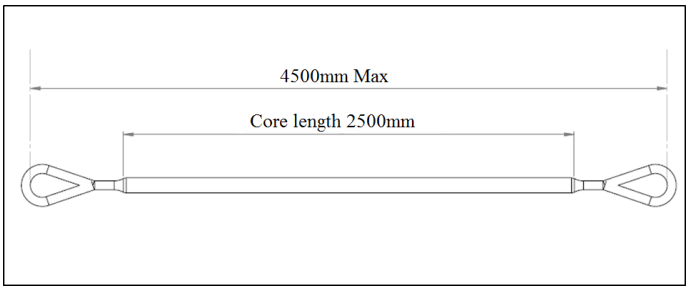

Figure 3: Working length and overall length of the P1 tethers.

Table 1: Construction of the P1 series prototypes detailed in this paper, core material as requested from supplier.

Prototype Number	Core material
P1-2	EPDM – 50A
P1-3	EPDM – 60A
P1-4	EPDM – 70A
P1-5	EPDM – 80A
P1-6	EPDM – 90A

4. METHODS

4.1 DUROMETER TESTING

The core elastomer material was supplied as five extruded round section lengths of 25 mm diameter having specified durometer hardness values of 50, 60, 70, 80 and 90 Shore A. A sample of 18 mm in length was cut from the middle part of each extrusion. The test end of each sample piece was polished using a wet 240 grit micro-section polishing wheel to produce a uniform flat surface. A Mitutoyo Hardmatic HH-331(A) durometer was used to take three readings for each test piece. Care was taken to distribute the three tests around the face of each test piece so as to avoid misrepresentation caused by slow material recovery after penetration of the indenter. Test indentations were made approximately 8 mm from the edge of the test face.

4.2 DYNAMIC MARINE COMPONENT TEST FACILITY

4.2 (a) Facility overview

The Dynamic Marine Component test facility (DMaC) is based in Falmouth Docks and is owned and operated by the University of Exeter. It is a large horizontal test machine that has a linear actuator and a two degrees of freedom headstock. Further specifications of DMaC and examples of other component tests are detailed in [15-17]. For the tether test work the headstock is not utilised and the linear actuator is used to provide displacement of up to 1000 mm and tension of up to 220 kN. The linear actuator follows a prescribed time series for either displacement or for tension and in both cases has full feedback control of the driving parameter.

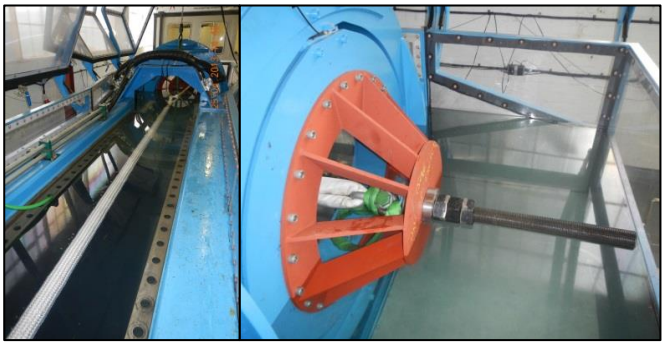

Figure 4: DMaC with a tether fitted and full of water (LH image). The pre-tension adjuster and 'top hat' (RH image).

The test piece can be submerged in fresh water which is essential for the tether test work in order that the assembly is properly lubricated. For the tether test work, an interchangeable headstock platen was manufactured that provided 800 mm of pre-tension travel via an M64 thread. The 'top hat' form of this platen also increases the effective test bed length of DMaC by 300 mm. Figure 4 shows DMaC with a tether assembly fitted ready to test (submerged in water) and the pre-tension adjuster providing maximum pre-tension. The pre-tension adjuster is important because it allows the slack to be removed from the test piece without using any

of the 1000 mm linear stroke available from the hydraulic ram.

4.2 (b) Calibration

DMaC was calibrated using a reference 5 tonne load cell which itself has calibration traceable to national standards. The results of the final DMaC calibration run are given in Figure 5.

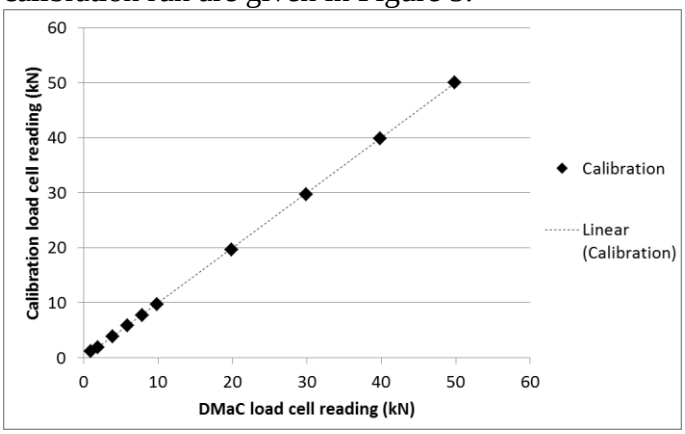

Figure 5: Final calibration run of DMaC using 5T reference load cell

A line of best fit has been fitted to the data points in the final calibration run which has a very good fit (the square of the Pearson product moment correlation coefficient, R^2 = 0.9999). A perfect correlation between the two load cells is achieved if the line of best fit has the form $y = x$. The equation for the line in the final calibration run here is:

$$y = 1.0016x - 0.0752$$

Applying this linear relationship to the range of loads investigated in the test work reported below provides a maximum error of + / - 0.07kN.

4.3 EYE SPLICE EXTENSION TESTS

The extension data output by DMaC relates to the extension of the entire tether rather than the working length. It is therefore necessary to quantify the axial stiffness of the eye splice terminations so that the extension of the eye splices can be subtracted from the total extension data to reveal the extension experienced by the working length of the tether.

Tests were performed on tethers P1-3 and P1-6 (after bedding in) using the displacement driven test ETT_08 (see Figure 6). A draw wire linear transducer was used to measure the extension between the connection shackle and the closest end of the working tether length. These tests were performed without submersion to eliminate the risk of water ingress and damage to the transducer.

4.4 PERFORMANCE TESTS REFERENCED TO A TENSION LOAD DATUM

A tension load datum might refer to the static pre-tension of a mooring line when the floating body is at calm and the tide height is at a minimum. A series of sine wave conditioning tests were run in force mode (the tension time series drives the linear actuator) to 'bed in' each tether. These conditioning tests are summarised in Table 2.

Table 2: Force mode conditioning test descriptions

Test I.D.	Pre-tension (kN)	Peak tension (kN)	Period (s)	Cycles (number)
ETT_03	1	10	8	10
ETT_04	2	20	8	10
ETT_05	2	40	8	5
ETT_06	2	60	8	5

Following completion of the conditioning tests the pre-tension was set to 1550 N and the tether was left at this tension for a prolonged period (overnight) to stabilise. At the end of this stabilisation period the pre-tension was reset to the tension datum (1550 N) if any drift had occurred. A displacement mode test (the displacement time series drives the linear actuator) was then conducted according to test script ETT_08. The drive data for this test is given in graphical form as Figure 6.

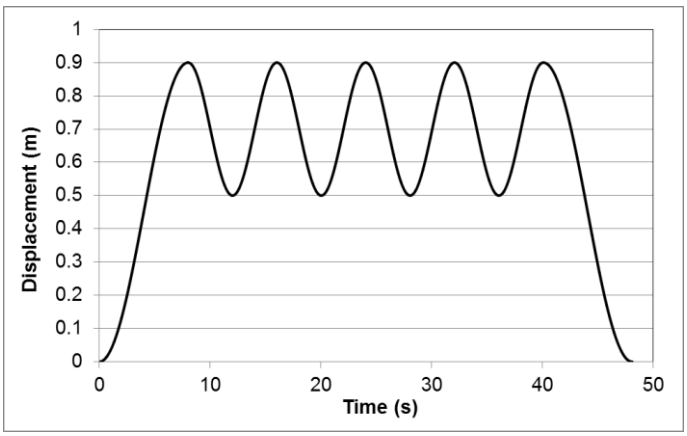

Figure 6: The displacement (extension) drive data for test ETT_08

4.5 PERFORMANCE TESTS REFERENCED TO A DISPLACEMENT DATUM

Referencing to a displacement datum allows for easier comparisons between the P1 tethers and conventional rope through comparison of calculated strain values.

The ETT_19 test was developed to extend the tether over the maximum achievable displacement range on DMaC (0-990mm). Tethers P1-2 and P1-6 were tested according to ETT_19. The test was conducted four times on each tether. Incremental increases in the test pre-tension were made up to a maximum possible pre-tension resulting from the full uptake of the adjuster thread.

4.6 FATIGUE ENDURANCE TEST

The current design stage of the tether aims to demonstrate and investigate the functional performance characteristics and does not yet address weaknesses related to fatigue and durability. However, this test stage was included to gain an early understanding of any critical weakness that might exist with the concept. To this end, a 'Thousand Cycle Load Limit' (TCLL) test was conducted on a single tether.

The TCLL test was developed by the Oil Company's International Marine Forum (OCIMF) to quantify mooring hawser response to tension - tension fatigue (cycling between lower and higher tension values) [18]. Here, the basic concepts of the TCLL test have been adapted to make it more appropriate for the P1 series tether and DMaC. These adaptations are associated with the frequency of cycling, the rate of increase of strain and the wetting of the test piece.

The tests load the tether cyclically for 1,000 cycles per test at increasing load steps, starting from 50% MBL, as detailed in Table 3. Short periods of static load are permitted between each test step, with the load always maintained above 1% MBL.
An adapted tether (P1-16) was prepared in order that the required loads could be achieved within the 1000 mm stroke available from DMaC.

The MBL for the tether was allocated a value of 220 kN based on the result of a breaking load test conducted on a representative tether in the previous stages of testing. Test scripts were prepared according to the outline structure detailed and these are listed in Table 3.

Table 3: Thousand cycle load limit test parameters. Constant values across all tests included 1% min load of 2.2 kN, sine wave period of 8 s and 1,000 cycles specified for each test.

Test I.D.	Peak load (% MBL)	Peak load (kN)
TETT_26	50	110
TETT_27	60	132
TETT_28	70	154
TETT_29	80	176

Conditioning test ETT_04 (Table 2) was performed twice to 'bed in' the tether and its connections before the TCLL sequence shown in Table 3 was initiated.

4.7 SEA TRIALS: SOUTH WEST MOORING TEST FACILITY (SWMTF)

Four tethers from the P1 test series, including P1-3 detailed in this paper, were deployed on a mooring limb at the South West Moorings Test Facility (SWMTF), Figure 7.

Figure 7: Four tethers for deployment (LH image). Tethers being deployed at SWMFT (RH image).

This UoE test facility is moored in Falmouth Bay and enables mooring systems and components to be exposed to representative sea conditions. Further details of the facility are provided in [17, 19]. This was intended to be an endurance test to indicate the durability of the tether when subjected to the marine environment with realistic mooring loads.

5. RESULTS

5.1 DUROMETER HARDNESS TESTS

Durometer hardness readings and mean results are given in Table 4.

Table 4: Durometer test results

Target Tether I.D.	Specified hardness (Shore A)	Hardness readings (Shore A)			Mean hardness (Shore A)
P1-2	50	54	54	54	54.0
P1-3	60	59	59	59	59.0
P1-4	70	70	71	71	70.7
P1-5	80	70	70	70	70.0
P1-6	90	81	80	81	80.7

From the results detailed above, it is clear that the EPDM used for both P1-5 and P1-6 was not as specified; P1-5 has been manufactured with 70A and P1-6 with 80A.

5.2 EYE SPLICE EXTENSION TESTS

Figure 8 shows the extension of a P1-3 eye splice recorded by the linear transducer over the five cycles of the ETT_08 test. The final sine wave is selected from the data set and the gradient from the cycle load up data (as shown by dotted line in Figure 8) is identified.

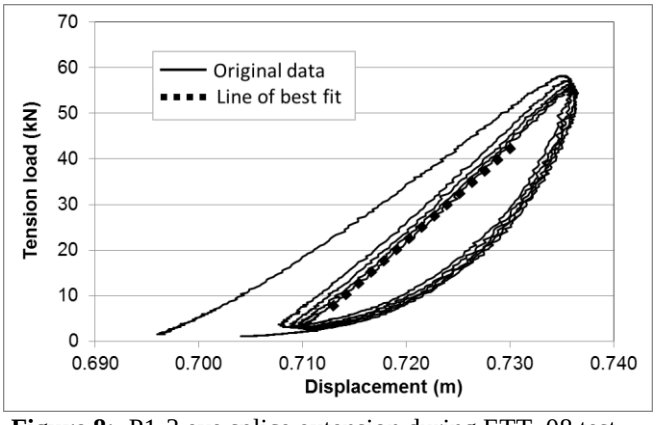

Figure 8: P1-3 eye splice extension during ETT_08 test.

This test and data analysis was repeated for P1-6 and the results are given in Table 5.

The mean value of 1965.93 kN/m was inverted to 5.09×10^{-4} m/kN and then doubled to 1.02×10^{-3} m/kN to approximate the total eye splice extension of a P1 series tether under load up conditions.

Table 5: Results of the eye splice extension tests (where R^2 value is the square of the Pearson product moment correlation coefficient)

Tether I.D.	Straight line gradient (kN/m)	R^2 value
P1-3 (single end)	2065.68	0.999
P1-6 (single end)	1866.18	0.999
Mean (single end)	1965.93	-

5.3 PERFORMANCE TESTS REFERENCED TO A TENSION LOAD DATUM

The final cycle (fifth cycle) load up data is identified. For each data time step, the incremental increase in tension is used to calculate the extension of the eye splices by applying the value 1.02×10^{-3} m/kN derived in section 5.2. The eye splice extension is then subtracted from each extension value recorded by DMaC to provide data corresponding to the extension of the working part of the tether. The extension is normalised against the original working length and expressed as a percentage. The tension load is normalised against the MBL of 220 kN (as detailed in section 4.6) and expressed as a percentage. Figure 9 shows the outcome of these tests in graphical form.

The divergence of the five plot lines demonstrates the differences in axial stiffness through the range of tethers. It is clear that in all cases the tether approximates a linear relationship between load and extension beyond a certain tension load. Figure 10 shows further analysis of this behaviour. In this figure, the final 20 data points have been clipped from each data set to remove a small portion of non-linear behaviour at the end of the load up cycle. This non-linear behaviour is caused by the viscous, time dependant properties of the elastomers as the displacement sine wave causes the stroke velocity to tend towards zero.

To establish the equation for the best fit straight line representing the near linear portion, an R^2 value (the square of the Pearson product moment correlation coefficient) of 0.9995 was sought. Starting at the origin end of each data set, data points were removed until the linear regression achieved an R^2 of 0.9995. The equation for this line was then detailed; the crucial value being the gradient, as this represents the tether axial stiffness, the crucial property under investigation.

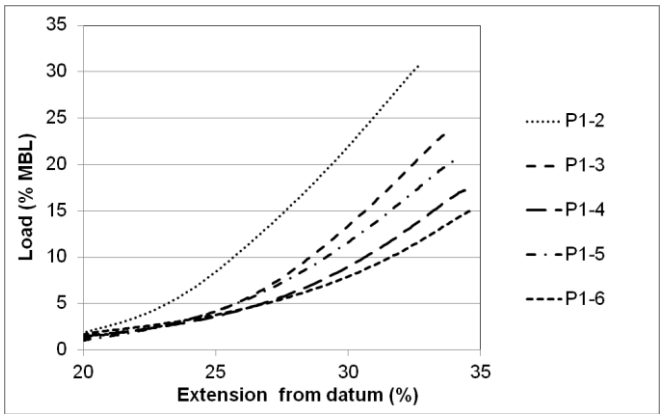

Figure 9: P1 series tether extension properties from a 1550 N pre-tension datum.

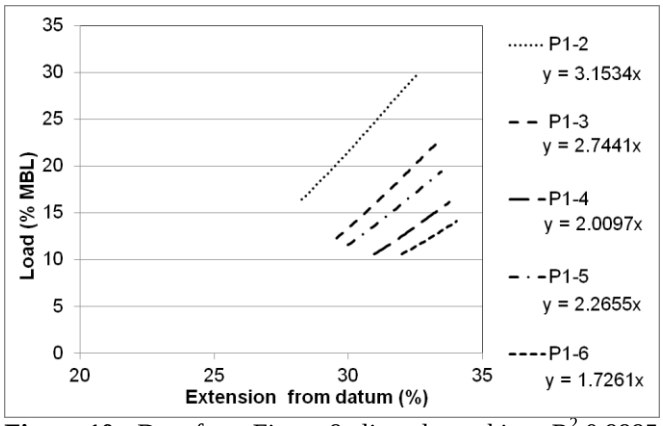

Figure 10: Data from Figure 9 clipped to achieve R^2 0.9995 linear regressions.

The gradient of the best fit straight line is shown in Figure 10 and these values are repeated in Table 6. The tethers are ranked according to their gradient and it is apparent that there is a relationship between the durometer hardness of the elastomer and the gradient. It should be noted that the stiffest tether is achieved with the softest core material and the most compliant tether, with the hardest core material.

Table 6: Tabulated results of the linear regressions shown in Figure 10.

Hardness (Shore A)	Tether	Gradient	Stiffness ranking
54	P1-2	y = 3.1534x	1
59	P1-3	y = 2.7441x	2
70	P1-5	y = 2.2655x	3
71	P1-4	y = 2.0097x	4
81	P1-6	y = 1.7261x	5

5.4 PERFORMANCE TESTS REFERENCED TO A DISPLACEMENT DATUM

The final cycle (fifth cycle) load up data is identified. In these tests a linear transducer recorded extension of the eye splice at one end of the tether. For each data point, the single eye splice extension result was doubled to approximate the total eye splice extension. This value was then subtracted from the total tether extension recorded by DMaC to derive the extension of the working part of the tether.

The tethers yield significantly upon initial loading, taking on a temporary extension 'set'. For this analysis, the extension results are referenced to a 'dynamic zero load length' that better represents the free length of the tether during cyclic loading. This free length is derived from a simple static load vs extension graph for each tether. The equation of the best fit straight line is then applied to the load recorded at the first data point to derive the corresponding extension.

The tension load for the tethers is referenced against an MBL of 220 kN based on a previous breaking load test on a representative tether (section 4.6). This allows load to be plotted as % of MBL for direct comparison to other ropes.

Figure 11 details the extension properties for the tethers tested alongside a reference rope; a double braid polyester rope (data obtained from Lankhorst Ropes).

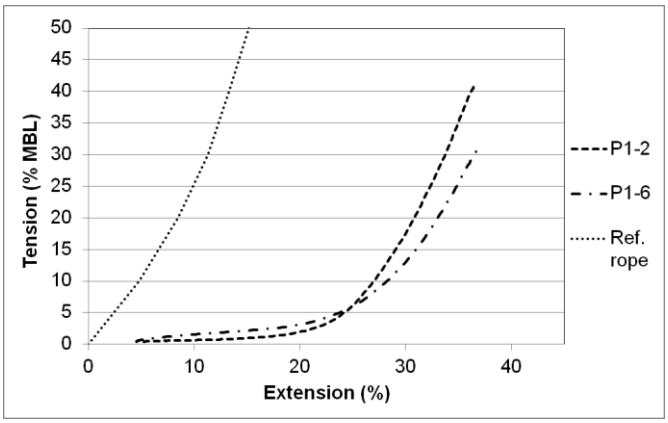

Figure 11: Normalised extension properties shown together with a reference rope.

The P1 series prototypes exhibit two phases of extension with an intermediate transition phase.

5.5 FATIGUE ENDURANCE TEST

The tether failed during TETT 28 (a load range of 1% - 70% MBL or 2.2 – 154 kN) at approximately the 187th cycle. The calculation for the thousand cycle load level is detailed in [18]:

$$TCLL = 100\% - \frac{6.91(100\% - TLL)}{Ln\ CTF} = 60.37\ \%$$

Where, TLL = test load level at which cycles to failure was determined
CTF = cycles to failure at test load level
6.91 = natural logarithm of 1000

Further work is required to understand the TCLL value in relation to other mooring options. Some publications suggest a TCLL of just 52% for polypropylene ropes [20]; however improvements in rope technology are now producing ropes with TCLL values approaching 80% [20, 21]. For an early proof of concept prototype 60% is an acceptable TCLL with clear potential for improvement in subsequent prototypes.

The failure (parting of strands) occurred at the point where the rope increases in diameter to envelop the core bundle. The edge of the core bundle caused fretting which is likely to have promoted this failure, shown in Figure 12.

Figure 12: Failed tether under fatigue cycle loading

Minor changes to the geometry of the core, such as a more gradual slope from the full diameter bundle to the empty rope will reduce the fretting in this area and lead to an improved TCLL value. Other variations on membrane could also be trialled to reduce friction at this point. As previously mentioned the P1 series tethers were designed as a proof of concept and durability was not a main objective at this stage.

A key feature of the Exeter Tether is the ability to specify axial stiffness and the fatigue endurance tests enabled improved understanding of how this property may change with longer term load cycling. By reviewing the slope of the load/displacement graph at various cycles throughout the testing the axial stiffness of the tether was shown to be relatively stable. The initial expected increase in stiffness stabilises at higher cycle numbers. The two phases of extension as detailed in section 5.4 remain observable into the last few cycles before failure. The test has proved the stiffness of the tether at design can be maintained under cyclical loading, and will not degrade; this has been shown up to 2,000 cycles and the stiffness of the system is relatively stable at this level of load cycling.

5.6 SEA TRIALS: SOUTH WEST MOORING TEST FACILITY (SWMTF)

Following a continuous testing period of nearly 6 months, the four tethers were recovered on 26th November 2013. Visually, the tethers survived the sea trials intact. As expected, significant marine growth developed on the tethers which varied depending on the depth of the tether during the deployment. Following basic cleaning with a brush and fresh water, there was no evidence of fretting or degradation other than a noticeable colour change to the rope. Following the recovery, further performance tests were conducted on the tethers which will be reported in subsequent publications.

6. CONCLUSIONS

The results described here prove the working concept of the Exeter Tether. The tether successfully de-couples the extension properties from the MBL of the load carrier. In so doing, the tether allows the selection, between certain limits, of axial stiffness for a given MBL. The tether is shown to have satisfactory load carrying capability and durability for this prototype stage of its development.

During tests, the tether displayed two phases of extension, each phase having a distinct axial stiffness. The two phases are separated by a smooth transition phase. The initial phase is one that provides soft extension properties up to a load

limit of around 5% of MBL. The second phase of extension displays a markedly stiffer behaviour but remains less stiff than a double braid rope of the same material.

The stiffness of the second phase is shown to be inversely related to the durometer hardness of the core material. Further analysis indicates that this result is related to the Poisson's ratio of the materials. This work needs to be progressed further before it can be reported.

Strain values in excess of 0.35 (35% extension) are shown to be achievable whilst remaining below 30% MBL. This is more than three times greater than the strain value achievable at 30% MBL for a conventional double braid rope of the same material.

These results demonstrate that the Exeter Tether has the potential to mitigate the conflict between axial stiffness and MBL discussed in the introduction. This will enable mooring designers to achieve a more compliant mooring design thus reducing peak and fatigue loads and subsequently reducing the costs of all structural elements within the system. Further work is ongoing to quantify the reductions in peak line loads possible through use of the tether and this will be reported in subsequent publications.

ACKNOWLEDGEMENTS

The authors gratefully acknowledge the support of Lankhorst Ropes who collaborated with the UoE to conduct the proof of concept study. The authors would also like to acknowledge the support of the UK Centre for Marine Energy Research (UKCMER) through the SuperGen programme funded by the EPSRC. Support from IFREMER's Materials in a Marine Environment Laboratory is also gratefully acknowledged.

REFERENCES

[1] Johanning L and Wolfram J (2005). *Challenging tasks on moorings for floating WECs*. in *Proceedings of the International Symposium on Fluid Machinery for Wave and Tidal Energy (IMechE)*. London, UK.

[2] Johanning L, Smith G, and Wolfram J (2005). *Towards design standards for WEC moorings*. in *Proc 6th European Wave Tidal Energy Conf.* Glasgow.

[3] Johanning L, Smith G H, and Wolfram J (2007). *Measurements of static and dynamic mooring line damping and their importance for floating WEC devices.* Ocean Engineering, **34**(14): p. 1918-1934.

[4] Harris R E, Johanning L, and Wolfram J (2004). *Mooring systems for wave energy converters: A review of design issues and choices.* Marec2004.

[5] Joosten H (2006). *Elastic mooring of navigation buoys.* International ocean systems, **10**(5): p. 16.

[6] Musial W, Butterfield S, and Boone A (2004). *Feasibility of Floating Platform Systems for Wind Turbines.* in *23rd ASME Wind Energy Symposium*: Reno, NV.

[7] Bachynski E E and Moan T (2012). *Design considerations for tension leg platform wind turbines.* Marine Structures, **29**(1): p. 89-114.

[8] Bengtsson N and Ekström V (2010). *Seaflex. The buoy mooring system: Increase life cycle and decrease cost for navigation buoys. Technical report.*

[9] McEvoy P (2012). *Combined elastomeric and thermoplasit mooring tethers.* in *4th Int. Conf. on Ocean Energy*: Dublin, Ireland.

[10] Thies P R, Johanning L, and McEvoy P (2014). *A novel mooring tether for peak load mitigation: Performance and service simulation testing - DRAFT.* International Journal of marine energy.

[11] Oil Companies International Marine Forum (2005). *Effective Mooring: Your guide to mooring equipment and operations*. 2nd edition ed: Witherby's Publishing.

[12] McKenna H A, Hearle J W S, and O'Hear N (2000). *Handbook of fibre rope technology*: Woodhead Publishing in Textiles.

[13] Parish D and Johanning L (2011). *International Patent Application Pub. No. WO 2011/089545 A1*. World Intellectual Property Oragniazation.

[14] Parish D and Johanning L (2012). *Mooring limb. US Patent Application Pub. No. US 2012/0298028 A1*.

[15] Johanning L, Thies P R, and Smith G H (2010). *Component test facilities for marine renewable energy converters.* in *Marine Renwable & Offshore Wind Energy Conference*: London

[16] Thies P R and Johanning L (2010). *Development of a marine component testing facility for marine energy converters.*

[17] Weller S D, et al. (2014). *Navigating the valley of death: Reducing reliability uncertainties for marine renewable energy.* in *ASRSNet International Conference*: Glasgow.

[18] Oil Companies International Marine Forum (2000). *Guidelines for the purchasing and testing of SPM hawsers*: Witherby and Co. Ltd.

[19] Johanning L, Spargo A, and Parish D (2008). *Large scale mooring test facility: A technical note*. in *Proc. of 2nd Int. conference on Ocean Energy (ICOE), Brest, France*. Brest, France.

[20] Baaj H P (2011). *Maritime Ropes Brieing 1/2011*. Lankhorst Ropes.

[21] Ropes L (2008). *High performance ropes EUROFLEX (catalouge extract).*